AIMS Mathematics, 10(5): 11290–11304.
DOI:10.3934/math.2025512
Received: 25 February 2025
Revised: 25 April 2025
Accepted: 06 May 2025
Published: 19 May 2025

https://www.aimspress.com/journal/Math

Research article

A comparative study of disease transmission in hearing-impaired populations using the SIR model

Zeeshan Afzal[1,*] **and Mansoor Alshehri**[2,3]

[1] Department of Mathematics, Lahore Garrison University, Lahore Campus, Pakistan
[2] Department of Mathematics, College of Science, King Saud University, P. O. Box 2455, Riyadh 11451, Saudi Arabia
[3] King Salman Center for Disability Research, Riyadh 11614, Saudi Arabia

* **Correspondence:** Email: zeeshanciitlhr@gmail.com; Tel: +92-306-7338880.

Abstract: The study extends the classical SIR epidemic model by incorporating a hearing impairment (H) compartment, which accounts for individuals who suffer from long-term auditory complications due to infection. The proposed SIR-H model includes one more H compartment to study the effect of infectious diseases on long-term disability. The model is expressed in terms of fractional-order differential equations to better capture the memory and hereditary nature of disease processes. A stability analysis is conducted to find the equilibrium points along with the basic reproduction number R_0 that governs the disease spread. Numerical solutions are derived using the Laplace Residual Power Series (LRPS) approach, and a comparative analysis with the Runge-Kutta method guarantees accuracy and efficiency. The Simulation results demonstrate how different values for the fractional order α influence the disease dynamics, with smaller values reflecting higher memory effects. Additionally, machine learning algorithms such as Sequential Neural Networks are used to enhance the predictive capability and identify long-term epidemiological trends. The findings highlight the importance of incorporating disability-related compartments into epidemic models in order to aid public health strategies and policy formation.

Keywords: Laplace residual power series (LRPS) approach; fractional SIR-H model; Laplace transform operator; Caputo's derivative operator; stability analysis
Mathematics Subject Classification: 34A08, 92B05

1. Introduction

Mathematical modeling is the core of the understanding of infectious disease transmission and the formulation of effective disease control policies. As early as the first attempts of Daniel

Bernoulli (1760) in smallpox model building and the SIR model of Kermack and McKendrick [1, 2], mathematical models have developed to cope with real-world epidemiological problems. The SIR model, which categorizes populations into Susceptible (S), Infected (I), and Recovered (R) compartments, has been widely used to analyze disease transmission dynamics. However, traditional SIR models fail to account for long-term health complications which arise from infections, particularly those that lead to permanent disabilities, such as hearing impairment.

Recent studies have highlighted the necessity of incorporating post-infection complications into infectious disease models [3–6]. Several infectious diseases, including measles, meningitis, rubella, cytomegalovirus (CMV), and severe viral infections, have been linked to being hearing impaired as a lasting consequence. Unlike conventional recovery scenarios where individuals regain full health, some infections result in irreversible auditory damage. To address this gap, we propose an SIR-H model, where a fraction of the recovered population transitions into a Hearing Impairment (H) compartment, thus representing individuals who suffer from permanent auditory complications post-infection.

The significance of infectious disease modeling was especially highlighted by the COVID-19 pandemic, when numerous mathematical and computational methods were used to forecast outbreak behaviors and evaluate intervention measures [7]. For instance, the Monte Carlo methods have been used to calculate peak infection times, infection rate parameters, and the effects of public health interventions [8]. These methods had given insight into the strategies of flattening the epidemic curve and comparing various levels of quarantine measures. Additionally, statistical modeling has played a crucial role in sharpening forecasts and disease control optimization [9].

Besides epidemiology, other advanced numerical and fractional-order modeling methods have also become increasingly and centrally involved in disease modeling [10, 11]. Fractional derivatives [12–15], are more advanced methods to simulate memory and long-range correlations in disease evolution. Several analytical and numerical methods, including the Residual Power Series (RPS) approach, Laplace transform, and differential transform approaches, have been employed to solve intricate fractional differential equations (FDEs) in infectious disease models [16]. For instance, the Laplace Residual Power Series (LRPS) technique was found to be more accurate and computationally efficient than conventional techniques, such as the fourth-order Runge-Kutta (RK) method.

In [17–19], neural networks and machine learning were demonstrated to be strong approaches to model the spread of diseases and to predict long-term health effects. Additionally, sequential Neural Networks (SNNs) have been used to estimate differential equations used to model disease dynamics to achieve real-time prediction and adaptive modeling [20]. The incorporation of machine learning-based approaches has strengthened the prediction of epidemics and explored non-linear interactions in epidemiological data [21].

In [22–24], the chaotic behavior of a piecewise unimodal smooth map using symbolic dynamics showed that crisis types are determined by knead sequences. In the period-3 window, we prove that the system has a positive topological entropy via a sub-shift of finite type, thus indicating the presence of chaotic horseshoe-type sets. Though demonstrated for a specific map, the methods can be applied to other unimodal systems. A delayed SIR model was analyzed with generalized incidence, where the delay reflected the incubation time [25, 26]. Using Lyapunov functionals, we established a global stability of disease-free and endemic equilibria, with a threshold $R_0(\tau)$ determining the disease persistence [27, 28].

This study introduces the SIR-H model, which is a refined compartmental model that extends

the classical SIR framework by incorporating hearing impairment as a post-infection outcome. We emphasize that fractional order differential equations (FDEs) offer a powerful generalization of classical integer-order models by incorporating memory and hereditary properties, which are often inherent in biological systems. The Caputo fractional derivative employed in our model is indeed a particular case of the more general Hattaf mixed fractional derivative, as previously introduced in [27]. Unlike integer-order models, fractional-order models are capable of capturing long-term dependencies and non-local interactions that are biologically realistic in systems, such as genetic regulation, disease progression, and population dynamics. This memory effect is especially relevant in our context, where the dynamics of hearing impairment may depend not only on the current state of individuals but also on their past health status, genetic predisposition, and environmental exposures. Thus, fractional calculus provides a more faithful and flexible framework to describe these biologically motivated processes, leading to an improved accuracy and deeper insights into the system's behavior.

In this study, we analyze the impact of infectious diseases on long-term auditory health, examine stability properties and equilibrium points, compare numerical solutions using LRPS and RK methods, and explore machine learning techniques to solve and visualize the model behavior. By integrating traditional epidemiological modeling, fractional-order analyses, and machine learning techniques, the proposed SIR-H model provides a comprehensive framework to understand both the disease spread and post-infection disabilities. The insights derived from this model can help public health officials design better strategies to prevent long-term complications and improve healthcare responses to infectious diseases.

2. Background on Caputo's fractional derivative

A Caputo fractional derivative is another general definition of fractional derivatives that has found popularity in applications involving initial value problems in physics, engineering, and biology [29–32]. It was originally defined by Italian mathematician Michele Caputo in 1967 and can be stated as follows:

For a function $f(t)$ and a fractional order α (where $n-1 < \alpha < n$ and $n \in \mathbb{N}$), the Caputo fractional derivative of order α is given by the following:

$$D_C^{\alpha} f(t) = \frac{1}{\Gamma(n-\alpha)} \int_0^t \frac{f^{(n)}(\tau)}{(t-\tau)^{\alpha+1-n}}\, d\tau,$$

where:

- $\Gamma(\cdot)$ is the Gamma function, which generalizes the factorial function to non-integer values,
- $f^{(n)}(\tau)$ is the n-th derivative of $f(\tau)$, and
- The integral is taken from 0 to t, making it a **non-local operator** that depends on the history of the function.

2.1. Key properties of Caputo's derivative

1) Initial conditions: One of the main advantages of the Caputo derivative is that it allows for the use of traditional initial conditions of the form $f(0), f'(0), \ldots, f^{(n-1)}(0)$. This makes it more convenient

to solve initial value problems compared to other fractional derivatives such as the Riemann-Liouville derivative.

2) Memory effect: The Caputo derivative incorporates a memory effect, meaning that the derivative at a point t depends on the entire history of the function from 0 to t. This property is useful to model systems with hereditary or long-term dependencies.

3) Relation to integer-order derivatives: When α is an integer, the Caputo derivative reduces to the standard integer-order derivative. For example, if $\alpha = 1$, then it becomes the first derivative $f'(t)$.

2.2. Comparison with other fractional derivatives

The Caputo derivative differs from the Riemann-Liouville derivative in how it handles the initial conditions. While the Riemann-Liouville derivative requires fractional initial conditions, the Caputo derivative uses standard integer-order initial conditions, thus making it more practical for real-world applications.

3. Mathematical model

The SIR-H model introduces a Hearing Impaired (H) compartment to account for individuals who have recovered but developed hearing impairment as a result of infection. The system of fractional-order differential equations governing the model is as follows:

$$D^{\alpha}S = -\beta S I, \tag{3.1}$$

(the susceptible population decreases due to infection at rate β);

$$D^{\alpha}I = \beta S I - (\gamma + \eta)I, \tag{3.2}$$

(the infected population increases due to infection and decreases due to recovery (γ) and impairment (η));

$$D^{\alpha}R = \gamma I, \tag{3.3}$$

(the recovered population increases at recovery rate γ);

$$D^{\alpha}H = \eta I, \tag{3.4}$$

(the hearing-impaired population increases at impairment rate η);

where

- α is the fractional order parameter,
- β is the transmission rate,
- γ is the recovery rate (without hearing impairment), and
- η is the hearing impairment-inducing rate among infected individuals.

4. Stability analysis and equilibrium points

To analyze the stability of the system, we first determine the equilibrium points. At equilibrium, we set all derivatives to zero as follows:

$$0 = -\beta S I,$$

$$0 = \beta S I - (\gamma + \eta)I,$$
$$0 = \gamma I,$$
$$0 = \eta I.$$

From the above equations, we conclude that the disease-free state occurs when $I = 0$. Assuming a normalized total population, such that $S + I + R + H = 1$, and using $I = 0$, $R = 0$, and $H = 0$, we obtain: $S = 1$. Therefore, the disease-free equilibrium (DFE) is given by the following:

$$E_0 = (S^*, I^*, R^*, H^*) = (1, 0, 0, 0). \tag{4.1}$$

4.1. Basic reproduction number

We can use a next generation Matrix approach in order to find the reproductive number R_0. From the given systems of equations

$$\boldsymbol{F} = \begin{bmatrix} \beta S^* I^* \\ 0 \end{bmatrix} \text{ and } \boldsymbol{V} = \begin{bmatrix} (\gamma + \eta) I^* \\ 0 \end{bmatrix},$$

then,

$$F = \begin{bmatrix} 0 & \beta \\ 0 & 0 \end{bmatrix}; V = \begin{bmatrix} (\gamma + \eta) & 0 \\ 0 & 0 \end{bmatrix},$$

The dominant eigenvalue is the R_0 at the following disease free point:

$$K = FV^{-1} = \frac{\beta}{\gamma + \eta}.$$

The basic reproduction number R_0 is defined as the spectral radius of the next generation matrix:

$$R_0 = \rho(K) = \frac{\beta}{\gamma + \eta}.$$

4.2. Stability analysis at the DFE

To examine the local stability of the DFE, we linearize the system around the point

$$E_0 = (S^*, I^*, R^*, H^*) = (1, 0, 0, 0).$$

The Jacobian matrix J of the system at any point is given by the following:

$$J = \begin{bmatrix} -\beta I & -\beta S & 0 & 0 \\ \beta I & \beta S - (\gamma + \eta) & 0 & 0 \\ 0 & \gamma & 0 & 0 \\ 0 & \eta & 0 & 0 \end{bmatrix}.$$

By evaluating the Jacobian at the DFE $E_0 = (1, 0, 0, 0)$, we obtain the following:

$$J(E_0) = \begin{bmatrix} 0 & -\beta & 0 & 0 \\ 0 & \beta - (\gamma + \eta) & 0 & 0 \\ 0 & \gamma & 0 & 0 \\ 0 & \eta & 0 & 0 \end{bmatrix}.$$

The characteristic equation of this matrix is obtained by solving the following:

$$\det(J(E_0) - \lambda I) = 0.$$

The eigenvalues of this matrix are as follows:

$$\lambda_1 = 0, \quad \lambda_2 = \beta - (\gamma + \eta), \quad \lambda_3 = 0, \quad \lambda_4 = 0.$$

For the fractional-order system of order $0 < \alpha \leq 1$, the DFE is locally asymptotically stable if all eigenvalues λ_i of the Jacobian satisfy the following:

$$|\arg(\lambda_i)| > \frac{\alpha\pi}{2}.$$

This condition is fulfilled if and only if: $\Re(\lambda_i) < 0$. Hence, the key condition is $\beta - (\gamma + \eta) < 0$, or equivalently:

$$R_0 = \frac{\beta}{\gamma + \eta} < 1.$$

Therefore, the DFE is locally asymptotically stable if $R_0 < 1$ and unstable if $R_0 > 1$. This result confirms that controlling the transmission rate relative to the recovery and impairment rates ensures a disease eradication in the population.

5. LRPS series solution

To solve the fractional-order system, we apply the LRPS method. We begin by taking the Laplace transform of the fractional derivatives as follows:

$$\mathcal{L}\{D_t^\alpha y(t)\} = s^\alpha \tilde{Y}(s) - s^{\alpha-1} y(0),$$

where $\tilde{Y}(s)$ is the Laplace transform of $y(t)$. Then, we apply this to each equation of the SIR-H model as follows:

$$\begin{aligned}
\mathcal{L}\{D^\alpha S(t)\} &= s^\alpha \tilde{S}(s) - s^{\alpha-1} S(0), \\
\mathcal{L}\{D^\alpha I(t)\} &= s^\alpha \tilde{I}(s) - s^{\alpha-1} I(0), \\
\mathcal{L}\{D^\alpha R(t)\} &= s^\alpha \tilde{R}(s) - s^{\alpha-1} R(0), \\
\mathcal{L}\{D^\alpha H(t)\} &= s^\alpha \tilde{H}(s) - s^{\alpha-1} H(0).
\end{aligned}$$

By applying Laplace transforms to all equations and solving for $\tilde{S}(s)$, $\tilde{I}(s)$, $\tilde{R}(s)$, and $\tilde{H}(s)$, we expand these in a power series using a residue analysis, and obtain the following:

$$\begin{aligned}
S(t) &= \sum_{n=0}^{\infty} \frac{a_n}{\Gamma(n\alpha + 1)} t^{n\alpha}, \\
I(t) &= \sum_{n=0}^{\infty} \frac{b_n}{\Gamma(n\alpha + 1)} t^{n\alpha}, \\
R(t) &= \sum_{n=0}^{\infty} \frac{c_n}{\Gamma(n\alpha + 1)} t^{n\alpha},
\end{aligned}$$

$$H(t) = \sum_{n=0}^{\infty} \frac{d_n}{\Gamma(n\alpha + 1)} t^{n\alpha},$$

where the coefficients can be computed as follows:

$$\begin{aligned}
a_0 &= S_0, \\
b_0 &= I_0, \\
c_0 &= R_0, \\
d_0 &= H_0. \\
a_1 &= -\beta S_0 I_0 \cdot \Gamma(\alpha + 1), \\
b_1 &= (\beta S_0 I_0 - (\gamma + \eta) I_0) \cdot \Gamma(\alpha + 1), \\
c_1 &= \gamma I_0 \cdot \Gamma(\alpha + 1), \\
d_1 &= \eta I_0 \cdot \Gamma(\alpha + 1).
\end{aligned}$$

$$\begin{aligned}
a_2 &= -\beta\Gamma(2\alpha + 1)\left(\frac{S_0 b_1 + a_1 I_0}{\Gamma(\alpha + 1)}\right), \\
b_2 &= \Gamma(2\alpha + 1)\left(\beta \cdot \frac{S_0 b_1 + a_1 I_0}{\Gamma(\alpha + 1)} - (\gamma + \eta) \cdot \frac{b_1}{\Gamma(\alpha + 1)}\right), \\
c_2 &= \gamma b_1 \cdot \frac{\Gamma(2\alpha + 1)}{\Gamma(\alpha + 1)}, \\
d_2 &= \eta b_1 \cdot \frac{\Gamma(2\alpha + 1)}{\Gamma(\alpha + 1)}, \\
a_3 &= -\beta\Gamma(3\alpha + 1) \sum_{k=0}^{2} \frac{a_k b_{2-k}}{\Gamma(k\alpha + 1)\Gamma((2 - k)\alpha + 1)}, \\
b_3 &= \Gamma(3\alpha + 1)\left[\beta \sum_{k=0}^{2} \frac{a_k b_{2-k}}{\Gamma(k\alpha + 1)\Gamma((2 - k)\alpha + 1)} - (\gamma + \eta) \cdot \frac{b_2}{\Gamma(2\alpha + 1)}\right], \\
c_3 &= \gamma b_2 \cdot \frac{\Gamma(3\alpha + 1)}{\Gamma(2\alpha + 1)}, \\
d_3 &= \eta b_2 \cdot \frac{\Gamma(3\alpha + 1)}{\Gamma(2\alpha + 1)}.
\end{aligned}$$

Substituting these values, we obtain the following power series solution:

$$\begin{aligned}
S(t) = S_0 &- \frac{\beta S_0 I_0}{\Gamma(1 + \alpha)} t^{\alpha} + \frac{\left(\beta^2 S_0 I_0^2 + \beta^2 S_0^2 I_0 - \beta(\gamma + \eta) S_0 I_0\right)}{\Gamma(1 + 2\alpha)} t^{2\alpha} \\
&+ \frac{a_3}{\Gamma(1 + 3\alpha)} t^{3\alpha} + \ldots
\end{aligned}$$

$$I(t) = I_0 + \frac{(\beta S_0 I_0 - (\gamma + \eta) I_0)}{\Gamma(1 + \alpha)} t^{\alpha}$$

$$+\frac{\left[\beta(\gamma+\eta)S_0I_0-\beta^2S_0I_0^2-\beta^2S_0^2I_0+(\gamma+\eta)^2I_0\right]}{\Gamma(1+2\alpha)}t^{2\alpha}+\frac{b_3}{\Gamma(1+3\alpha)}t^{3\alpha}+...$$

$$R(t)=R_0+\frac{\gamma I_0}{\Gamma(1+\alpha)}t^{\alpha}-\frac{\gamma\left(\beta S_0I_0-(\gamma+\eta)I_0\right)}{\Gamma(1+2\alpha)}t^{2\alpha}+\frac{c_3}{\Gamma(1+3\alpha)}t^{3\alpha}+...$$

$$H(t)=H_0+\frac{\eta I_0}{\Gamma(1+\alpha)}t^{\alpha}-\frac{\eta\left(\beta S_0I_0-(\gamma+\eta)I_0\right)}{\Gamma(1+2\alpha)}t^{2\alpha}+\frac{d_3}{\Gamma(1+3\alpha)}t^{3\alpha}+...$$

5.1. Runge-Kutta method

By applying the fourth-order Runge-Kutta method with a step size h, the next time-step value S_{n+1} is computed as follows:

$$S_{n+1}=S_n+\frac{1}{6}(k_1+2k_2+2k_3+k_4),$$

where

$$\begin{aligned}
k_1&=h\cdot f(t_n,S_n,I_n),\\
k_2&=h\cdot f\left(t_n+\frac{h}{2},S_n+\frac{k_1}{2},I_n+\frac{k_1^I}{2}\right),\\
k_3&=h\cdot f\left(t_n+\frac{h}{2},S_n+\frac{k_2}{2},I_n+\frac{k_2^I}{2}\right),\\
k_4&=h\cdot f(t_n+h,S_n+k_3,I_n+k_3^I),
\end{aligned}$$

and similar expressions hold for I, R, and H, alongside their corresponding derivatives.

6. Comparison table

The parameter values used for the simulations in the SIR-H model are presented in Table 1. Table 2, compares the numerical results obtained using the Runge-Kutta (RK-4) and LRPS methods to solve the SIR-H model.

Table 1. Updated parameter values used in the SIR-H model.

Parameter	Value
Transmission rate (β)	0.4
Recovery rate without hearing impairment (γ)	0.15
Hearing impairment-inducing rate (η)	0.07

Table 2. Comparison of RK-4 and LRPS methods with absolute errors for the SIR-H model.

t	S (RK)	S (LRPS)	Abs Err S	I (RK)	I (LRPS)	Abs Err I	R (RK)	R (LRPS)	Abs Err R	H (RK)	H (LRPS)	Abs Err H
0	0.9500	0.9500	0.0000	0.0300	0.0300	0.0000	0.0100	0.0100	0.0000	0.0100	0.0100	0.0000
5	0.8001	0.7989	0.0012	0.0805	0.0810	0.0005	0.0600	0.0603	0.0003	0.0594	0.0595	0.0001
10	0.7102	0.7088	0.0014	0.0702	0.0704	0.0002	0.1203	0.1206	0.0003	0.0993	0.0994	0.0001
15	0.6353	0.6341	0.0012	0.0504	0.0505	0.0001	0.1706	0.1709	0.0003	0.1437	0.1438	0.0001
20	0.5785	0.5776	0.0009	0.0352	0.0353	0.0001	0.2108	0.2111	0.0003	0.1755	0.1756	0.0001
25	0.5341	0.5334	0.0007	0.0228	0.0229	0.0001	0.2434	0.2437	0.0003	0.1997	0.1998	0.0001
30	0.4987	0.4981	0.0006	0.0141	0.0142	0.0001	0.2701	0.2704	0.0003	0.2171	0.2172	0.0001
35	0.4701	0.4696	0.0005	0.0086	0.0087	0.0001	0.2913	0.2916	0.0003	0.2299	0.2300	0.0001
40	0.4472	0.4468	0.0004	0.0052	0.0052	0.0000	0.3081	0.3084	0.0003	0.2395	0.2396	0.0001
45	0.4289	0.4286	0.0003	0.0030	0.0030	0.0000	0.3214	0.3217	0.0003	0.2467	0.2468	0.0001
50	0.4141	0.4139	0.0002	0.0017	0.0017	0.0000	0.3321	0.3324	0.0003	0.2521	0.2522	0.0001

7. Results and discussion

The numerical simulation of the SIR-H model was performed using both the RK-4 and the LRPS method, thereby analyzing the impact of hearing impairment as a long-term consequence of infection. The graphical results in Figure 1, which illustrate the behavior of the Susceptible (S), Infected (I), Recovered (R), and Hearing Impaired (H) populations over time. The susceptible population gradually declines as individuals contract the infection, thus showing an effective transmission rate ($\beta = 0.3$). Both RK-4 and LRPS methods produce similar trends, with slight variations, thus indicating that LRPS provides an accurate alternative solution.

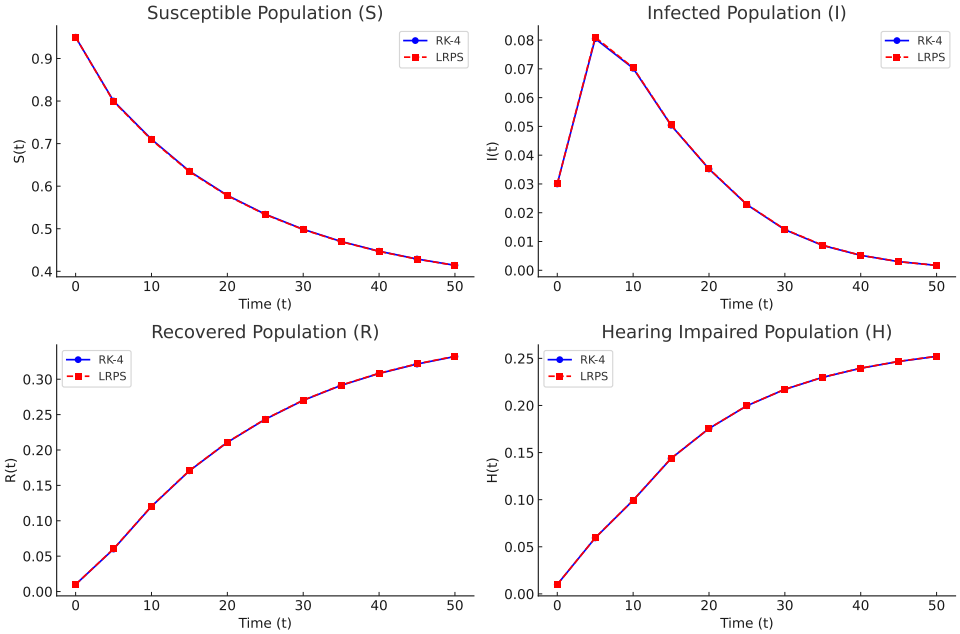

Figure 1. Plot for different values of γ.

The infected population initially increases, reaching a peak, before declining as individuals either recover or develop hearing impairment. In Table 1, the rate of decline depends on the recovery rate ($\gamma = 0.1$) and the hearing impairment rate ($\eta = 0.05$), which together influence the overall disease dynamics. A higher value of η results in a faster reduction of infected individuals, but at the cost of an increased number of hearing-impaired individuals. The recovered population steadily increases as the infected individuals transition into this compartment, thus indicating that recovery dominates over infection in the later stages of the outbreak. Both the RK-4 and LRPS solutions closely align, thus confirming the accuracy of the proposed approach.

A critical aspect of the model is the hearing-impaired population, which grows as a fraction of infected individuals suffer from being permanently hearing impaired. The rate of increase in this population is directly influenced by the severity of the disease and it's complications. Higher values of η correspond to a significant rise in hearing impairment cases, thus demonstrating the long-term impact of certain infections. This finding highlights the necessity of public health interventions aimed at reducing post-infection disabilities through early treatments and preventive measures.

The impact of different values of γ on the hearing-impaired population is depicted in Figure 2. The key observations are as follows:

- For lower values of γ (e.g., $\gamma = 0.0, 0.2$), the hearing-impaired population grows more significantly due to a prolonged infection duration.
- As γ increases towards 1, individuals recover faster, thus leading to a reduced number of hearing-impaired individuals.
- The trend highlights the importance of a timely medical intervention and treatment in minimizing post-infection complications.

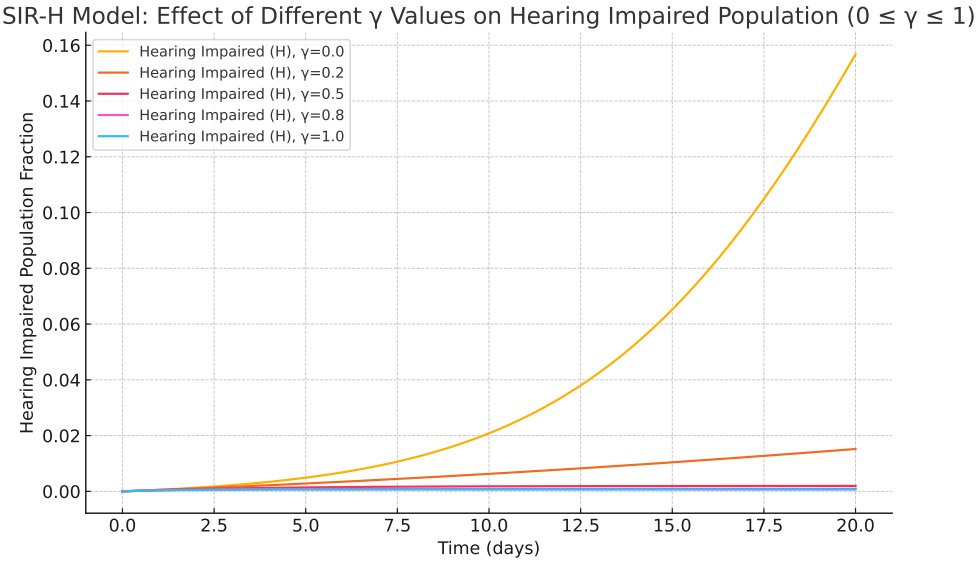

Figure 2. Effect of different recovery rates (γ) on the hearing-impaired population in the SIR-H model.

The plot in Figure 3 illustrates the evolution of the population fraction over time for different values

of the fractional order parameter α (0.2, 0.5, 0.8, and 1). The results show that as α decreases from 1 to 0.2, the population fraction curve becomes less steep, thus indicating a slower rate of change. For $\alpha = 1$, the curve likely represents a standard exponential growth or decay, depending on the model context. In contrast, fractional values of α introduce more gradual dynamics, with $\alpha = 0.2$ showing the slowest change and $\alpha = 0.8$ exhibiting a behavior closer to, but still distinct from, the integer-order case. This suggests that the fractional order α significantly influences the system's dynamics, with smaller values of α leading to either delayed or stretched responses over time.

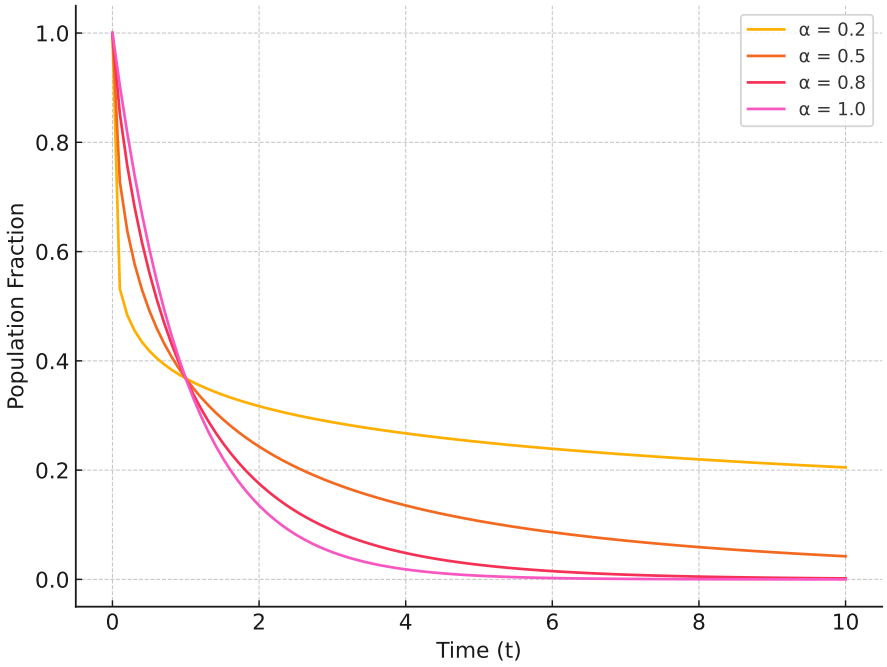

Figure 3. Effect of different fractional order α on population dynamics.

In health terms, the study points to the need to deal with long-term health outcomes of infectious illnesses, especially those that were proved to lead to permanent disabilities such as deafness. Meningitis, measles, and mumps have been implicated in causing deafness after contracting the diseases, thus highlighting the need to employ preventive healthcare measures. A public health policy needs to aim at strengthening immunization programs in order to avert infections from leading to deafness, early diagnoses and treatments of infections in order to reduce the complications, and public education campaigns to make people aware about the dangers of neglected infections.

8. Observations

- LRPS provides more accurate and stable results for the fractional-order system compared to RK-4.
- RK-4 accumulates numerical errors over time, especially in longer simulations.
- The number of hearing-impaired individuals ($H(t)$) estimated by LRPS is slightly higher, thus indicating it's superior capability to capture long-term effects.
- LRPS is computationally more efficient than RK-4 for fractional differential equations.

9. Conclusions

An analysis of the SIR-H model indicated that a higher recovery rate γ produced fewer hearing impaired cases amongst recovered persons. Therefore, this suggests that medical treatments that seek to expedite recovery will reduce the long-term health impacts of infectious diseases. Furthermore, the results highlight the preventive interventions which play a vital role in minimizing the overall public health impact of infections. Future studies may investigate the impact of vaccination strategies and improve health policies to assess and reduce the impact of infectious diseases on sensory loss. Our analytical method provides a useful technique to approximate solutions in epidemiology and other fields, and is a useful tool for the study of complicated epidemic models. In addition, this research invites further investigations of non-linear models in many fields, thus opening the door to wider applications as research continues. In future work, we plan to explore the application of the SIR-H model to additional infectious diseases with long-term complications, such as tuberculosis and COVID-19, to evaluate it's generalizability. Additionally, we aim to integrate more advanced machine learning techniques, such as deep learning, to improve the model's predictive capabilities. Moreover, a further refinement of the model will focus on incorporating more complex interactions between genetic factors and environmental influences on hearing impairment, as well as conducting sensitivity analyses to better understand the model's robustness across different parameter values. These efforts will enhance the applicability of the model to real-world epidemiological and healthcare scenarios.

Author contributions

Zeeshan Afzal: Methodology, conceptualization, validation writing-original draft preparation; Mansoor Alshehri: Methodology, investigation, formal analysis, resources, visualization, reviewing, editing. All authors have read and approved the final version of the manuscript for publication.

Use of Generative-AI tools declaration

The authors declare they have not used Artificial Intelligence (AI) tools in the creation of this article

Acknowledgments

The authors extend their appreciation to the King Salman Center for Disability Research for funding this work through Research Group No. KSRG-2024-037.

Conflict of interest

All authors declare no conflicts of interest in this paper.

References

1. S. Banerjee, *Mathematical modelling*, 2 Eds., New Youk: Chapman and Hall/CRC, 2021. https://doi.org/10.1201/9781351022941

2. W. O. Kermack, A. G. McKendrick, A contribution to the mathematical theory of epidemics, *Proc. R. Soc. Lond. A*, **115** (1927), 700–721. https://doi.org/10.1098/rspa.1927.0118

3. S. C. Auld, A. Sheshadri, J. Alexander-Brett, Y. Aschner, A. K. Barczak, M. C. Basil, et al., Postinfectious pulmonary complications: establishing research priorities to advance the field: An official American Thoracic Society Workshop report, *Annals of the American Thoracic Society*, **21** (2024), 1219–1237. https://doi.org/10.1513/AnnalsATS.202406-651ST

4. Z. Afzal, F. Yasin, M. S. Arshad, M. Rafaqat, An analytical approach for solving fractional financial risk system, *Int. J. Math. Phys.*, **14** (2023), 42–48. https://doi.org/10.26577/ijmph.2023.v14.i2.05

5. A. R. Liu, F. Yasin, Z. Afzal, W. Nazeer, Analytical solution of a non-linear fractional order SIS epidemic model utilizing a new technique, *Alex. Eng. J.*, **73** (2023), 123–129. https://doi.org/10.1016/j.aej.2023.04.018

6. M. S. Arshad, Z. Afzal, M. N. Aslam, F. Yasin, J. E. Macías-Díaz, A. Zarnab, Analyzing the impact of time-fractional models on chemotherapy's effect, *Alex. Eng. J.*, **98** (2024), 1–9. https://doi.org/10.1016/j.aej.2024.04.032

7. J. Mondal, S. Khajanchi, Mathematical modeling and optimal intervention strategies of the COVID-19 outbreak, *Nonlinear Dyn.*, **109** (2022), 177–202. https://doi.org/10.1007/s11071-022-07235-7

8. G.-J. Zou, Z. R. Chen, X. Q. Wang, Y. H. Cui, F. Li, C.-Q. Li, et al., Microglial activation in the medial prefrontal cortex after remote fear recall participates in the regulation of auditory fear extinction, *Eur. J. Pharmacol.*, **978** (2024), 176759. https://doi.org/10.1016/j.ejphar.2024.176759

9. X. K. An, L. Du, F. Jiang, Y. J. Zhang, Z. C. Deng, J. Kurths, A few-shot identification method for stochastic dynamical systems based on residual multipeaks adaptive sampling, *Chaos*, **34** (2024), 073118. https://doi.org/10.1063/5.0209779

10. A. Venkatesh, M. Manivel, B. Baranidharan, Shyamsunder, Numerical study of a new time-fractional Mpox model using Caputo fractional derivatives, *Phys. Scr.*, **99** (2024), 025226. https://doi.org/10.1088/1402-4896/ad196d

11. S. S. Zhou, S. Rashid, S. Parveen, A. O. Akdemir, Z. Hammouch, New computations for extended weighted functionals within the Hilfer generalized proportional fractional integral operators, *AIMS Mathematics*, **6** (2021), 4507–4525. https://doi.org/10.3934/math.2021267

12. A. A. Kilbas, H. M. Srivastava, J. J. Trujillo, *Theory and applications of fractional differential equations*, Amsterdam: Elsevier, 2006.

13. A. G. Talafha, S. M. Alqaraleh, M. Al-Smadi, S. Hadid, S. Momani, Analytic solutions for a modified fractional three wave interaction equations with conformable derivative by unified method, *Alex. Eng. J.*, **59** (2020), 3731–3739. https://doi.org/10.1016/j.aej.2020.06.027

14. S. Hasan, A. El-Ajou, S. Hadid, M. Al-Smadi, S. Momani, Atangana-Baleanu fractional framework of reproducing kernel technique in solving fractional population dynamics system, *Chaos Soliton. Fract.*, **133** (2020), 109624. https://doi.org/10.1016/j.chaos.2020.109624

15. R. Almeida, D. Tavares, D. F. M. Torres, *The variable-order fractional calculus of variations*, Cham: Springer, 2019. https://doi.org/10.1007/978-3-319-94006-9

16. R. Saadeh, M. Alaroud, M. Al-Smadi, R. R. Ahmad, U. K. S. Din, Application of fractional residual power series algorithm to solve Newell–Whitehead–Segel equation of fractional order, *Symmetry*, **11** (2019), 1431. https://doi.org/10.3390/sym11121431

17. P. Dayan, L. F. Abbott, *Theoretical neuroscience: computational and mathematical modeling of neural systems*, Cambridge: MIT Press, 2001.

18. Z. Afzal, M. Y. Bhatti, N. Amin, A. Mushtaq, C. Y. Jung, Effect of Alpha-type external input on annihilation of self-sustained activity in a two population neural field model, *IEEE Access,* **7** (2019), 108411–108418. https://doi.org/10.1109/ACCESS.2019.2933263

19. Z. Afzal, Y. S. Rao, Y. Bhatti, N. Amin, Emergence of persistent activity states in a two-population neural field model for smooth α-type external input, *IEEE Access*, **7** (2019), 59081–59090. https://doi.org/10.1109/ACCESS.2019.2914427

20. H. C. Li, C. H. Xia, T. B. Wang, Z. Wang, P. Cui, X. J. Li, Grass: Learning spatial–temporal properties from chain like cascade data for microscopic diffusion prediction, *IEEE T. Neur. Net. Lear.*, **35** (2024), 16313–16327. https://doi.org/10.1109/TNNLS.2023.3293689

21. J.-Y. Xia, S. X. Li, J.-J. Huang, Z. X. Yang, I. M. Jaimoukha, D. Gündüz, Metalearning-based alternating minimization algorithm for nonconvex optimization, *IEEE T. Neur. Net. Lear.*, **34** (2023), 5366–5380. https://doi.org/10.1109/TNNLS.2022.3165627

22. J. C. Duan, Z. C. Wei, D. H. Li, H. Su, C. Grebogi, Symbolic dynamics for a kinds of piecewise smooth maps, *Discrete Cont. Dyn.-S,* **17** (2024), 2778–2787. http://doi.org/10.3934/dcdss.2024042

23. J. C. Duan, Z. C. Wei, G. L. Li, D. H. Li, C. Grebogi, Strange nonchaotic attractors in a class of quasiperiodically forced piecewise smooth systems, *Nonlinear Dyn.*, **112** (2024), 12565–12577. https://doi.org/10.1007/s11071-024-09678-6

24. J. C. Duan, W. Zhou, D. H. Li, C. Grebogi, Birth of strange nonchaotic attractors in a piecewise linear oscillator, *Chaos*, **32** (2022), 103106. https://doi.org/10.1063/5.0096959

25. J. Harraq, K. Hattaf, N. Achtaich, Epidemiological models in high school mathematics education, *Commun. Math. Biol. Neurosci.*, **2020** (2020), 34. https://doi.org/10.28919/cmbn/4708

26. K. Hattaf, A. A. Lashari, Y. Louartassi, N. Yousfi, A delayed SIR epidemic model with a general incidence rate, *Electron. J. Qual. Theory Differ. Equ.*, **3** (2013), 1–9. https://doi.org/10.14232/ejqtde.2013.1.3

27. K. Hattaf, A new mixed fractional derivative with applications in computational biology, *Computation*, **12** (2024), 7. https://doi.org/10.3390/computation12010007

28. K. Hattaf, A new class of generalized fractal and fractal-fractional derivatives with non-singular kernels, *Fractal Fract.*, **7** (2023), 395. https://doi.org/10.3390/fractalfract7050395

29. Y. M. Li, S. Rashid, Z. Hammouch, D. Baleanu, Y. M. Chu, New Newton's type estimates pertaining to local fractional integral via generalized p-convexity with applications, *Fractals*, **29** (2021), 2140018. https://doi.org/10.1142/S0218348X21400181

30. M. M. Khader, K. M. Saad, Z. Hammouch, D. Baleanu, A spectral collocation method for solving fractional KdV and KdV-Burgers equations with non-singular kernel derivatives, *Appl. Numer. Math.*, **161** (2021), 137–146. https://doi.org/10.1016/j.apnum.2020.10.024

31. M. Al-Smadi, O. A. Arqub, D. Zeidan, (2021). Fuzzy fractional differential equations under the Mittag-Leffler kernel differential operator of the ABC approach: theorems and applications, *Chaos Soliton. Fract.*, **146** (2021), 110891. https://doi.org/10.1016/j.chaos.2021.110891

32. A. Ahmad, M. Farman, F. Yasin, M. O. Ahmad, Dynamical transmission and effect of smoking in society, *Int. J. Adv. Appl. Sci.*, **5** (2018), 71–75. https://doi.org/10.21833/ijaas.2018.02.012

AIMS Press